

# A High-Performance Reconfigurable Four Element Multiband MIMO Antenna for UWB Communications

<sup>1</sup>B. Santhikiran, <sup>2</sup>Dr. T. Kavitha

<sup>1</sup>Research scholar, Dept. of ECE,

Vel Tech Rangarajan Dr. Sagunthala R&D Institute of Science and Technology,  
Avadi, Chennai, Tamil Nadu. & Associate professor, Dept. of ECE, ALIET, Vijayawada, India

<sup>2</sup>Professor, Dept. of ECE,

Vel Tech Rangarajan Dr. Sagunthala R&D Institute of Science and Technology,  
Avadi, Chennai, Tamil Nadu, India

\*Corresponding Author Mail: shanthikiranshanthi@gmail.com

**Abstract:** For 5G applications, a 4-element orthogonal multi-input, multi-output antenna with an H-slot is advised. This antenna's CPW power source has four elements with better isolation. For this proposed antenna, the dimensions are reduced to  $80 \times 80 \times 1.6\text{mm}^3$ , and the band obstruction with a parameter less than -10dB that is from 2.2GHz to 20GHz and it notches vary from 3.4GHz to 4.3GHz in the frequency range of 8.2GHz to 8.7GHz. In order to support WiMAX (3.3GHz–3.7GHz) and band ranges from 8.2GHz–8.7GHz in military/radar applications, notched filters will be used. The proposed antenna proved successful in achieving mutual coupling at less than -19 dB. The antenna's ECC level is 0.019 and its directivity gain is almost 10 db, making it a very good antenna. Except at the notches, the peak gain and radiation efficacy are 5.8 dB and 82%, respectively. This suggested antenna can be used for UWB applications such location monitoring, communications, military/radar applications, and biomedical systems as a prepared option or recommendation.

**Keywords—:** Envelope Correlation Coefficient, Mutual Coupling, Co-planar waveguide Fed, Directivity Gain, MIMO.

## I. INTRODUCTION

Ultra-wideband antennas (UWB) are popular today because they have features like inexpensive cost, an incredibly fast data rate, and a lot of channel-to-channel communication. However, Multipath fading and dependability are disadvantages of UWB antennas. The UWB antenna's shortcomings can be fixed using this MIMO antenna.

Multiple antennas are used for communication by MIMO antennas. MIMO antennas improved communication by using multiple antennas both transmission as well as reception. These days, MIMO antennas are significantly important than ever thanks to features similar to more capacity, multipath fading, minimal co-channel interference, larger data speeds, or less signal noise. Because MIMO antennas have a strong mutual coupling effect, having a number of antennas in one building may cause antenna properties to degrade. It is possible to solve this issue by improving antenna separation.

The 5G antennas offer effective separation. Different WLAN (5.15 - 5.85 GHz), WiMAX (3.3 - 3.8 GHz), and X-Band communication satellite (7.99 - 8.4 GHz) kinds make up narrowband communication systems. Frequency bands are contained in existing frequency bands.

The development of MIMO antennas that operate at a Wideband spectrum frequency has improved the multi-path propagation fade problem and channel interference. Ultra-wideband (UWB) technology have drawn a lot of interest because of its inherent benefits, which include high-speed communication, remarkably low power consumption, and low cost. The Federal Communications Commission (FCC) permitted the usage of the frequency band in the range 3.1 - 10.6 GHz for UWB applications in 2002. Microstrip lines or Coplanar waveguide feeds were used in the UWB antenna design. Additionally, Wide bandwidth is one benefit of CPW-fed antennas, and they also have less loss than microstrip line antenna arrays. Various methods for creating compact MIMO structures have been developed for numerous MIMO systems. The transceivers were arranged parallel to one another, just as the original MIMO antenna we presented. The interrelated ground antenna elements are placed orthogonally to one another. In MIMO technology, other methods are also utilized to lessen the mutual interference between both antenna elements. These methods include the usage of EBG structures, DGS structures, and meta-material structures.

At the appropriate frequencies, this proposed antenna produced satisfactory isolation. This antenna has both triple

and dual notches. A 4-orthogonal MIMO antenna is employed in this study. This antenna includes dual-notch functionality for several bands with coupling of under -15dB. WiMAX bands are used for single MIMO, dual MIMO WLAN bands, in addition to triple notch MIMO UWB bands also suggested. The authors have suggested a MIMO antenna array with dual notches and an F-shaped stub for impulse radio UWB uses where excellent isolation is offered in prior publications. It is advised to use a 4-element MIMO antenna including collinear and orthogonal elements.

The paper is structured as follows: part 1 shows the introduction part; Section 2 talks about the literature analysis for this study. Discussion of single and dual antennas with geometrical parameters is covered in Session 3. Section 4 presents the results. The conclusion of the work is covered in more detail in Session 6. It includes the paper's four structural components.

## II. LITERATURE SURVEY

Tiwari, R.N., et al. [17] reported an eliminating technique-based two or four port maximum divergence MIMO antenna system for UWB communication in 2019. In this study, two distinct multiple-output (MIMO) antennas that are lightweight and portable are designed and built for usage in applications based on ultra-wideband. Use of the neutralisation line method considerably reduces the admittance among the two spreading patches. The measured (antenna) real gain from radiation efficiency varies between 0.95dB to 2.91dB from 70.01 % to 79.87 %, correspondingly, across the whole frequency spectrum. It offers a smaller bandwidth and a higher antenna gain.

A CPW-fed MIMO antenna system for ultra-wideband communications was presented by A. Dkiouak et al. [18] in 2020. In this study, a compressed MIMO antenna with high isolation was created for use in UWB applications. The intended antenna comprises of dual parallel-to-ones another, identical monopoles (CPW) supplied via a 50 ohm coplanar tunnel. The MIMO antenna has a total size of 36 x 36 x 1.6 mm<sup>3</sup> and is constructed on reduced fire retardants 4 (FR4) foundations. The wideband characteristic impedance of the planned antenna is satisfactory. The developed antenna performs well and UWB applications improve with such an efficient antenna because it has a DG (diversity gain) of above 9.9 dB and the ECC (envelope correlation coefficient) of below 0.01.

Naktong, W., et al. presented rectangular four-port monopole antennas with UWB MIMO use in 2020 [19]. The proposed antenna was built with stepwise etching merely on the ground

plane with radiating patch for arrow-shaped slots etching in order to boost bandwidth and increase performance. Multiple antenna elements' mutual coupling was reduced by using homogeneous components and angular variation approaches. The Computer Simulation Technology program (CST) was utilized in the structural simulation technique to examine the antenna properties, including the radiation patterns, mutual coupling, group delay, and envelope correlation coefficient. Bidirectional radiation was present. The four-port antenna's efficiency was also more than 85.70%, and the antenna gain was quite low.

For UWB MIMO applications, Sediq, H.T., et al. [20] proposed an epsilon-shaped ripple antenna in 2022. This work describes a unique epsilon-shaped geometry-based flat ultra-wideband (UWB) ripple antenna for microwave applications. All smart antenna geometry is anticipated by merging the four epsilon forms with a trio of straight-line conductors. The total dimensions of the MIMO antenna are 26 mm by 36 mm. The impedance bandwidth of 2.26 to 18.05 GHz is included in the new configuration. The suggested antenna has a reduced antenna size and a maximum of 7.81 dB gain for a working bandwidth of 18.01 GHz.

A compact 2 different MIMO antenna and a four-port MIMO antenna were described in 2022 by Sathiyapriya, T., et al., [21] and are intended to enhance the isolation characteristics for ultra-wideband (UWB) communication. In order to lessen reciprocal coupling between radiating elements, the circular neutralizer can be used as a decoupling structure. The overall dimensions of the proposed hybrid plus multiple antennas are 21 mm and 31 mm and 48 mm and 31 mm, correspondingly. Antenna design is done on the FR4 the substrate, which is approximately 1.6 mm thickness. In a range between 3.1 GHz - 10.6 GHz frequency, increased isolation is feasible to a maximum of 29 dB with the appropriate impedance. The proposed UWB antenna provides a decent antenna size with a narrower bandwidth.

## III. SINGLE ELEMENT

A monopole antenna with shorter edges and a gap sleeve is built in Figure 1. This monopole antenna receives power from a (CPW) coplanar waveguide. The fundamental equations using CPW feeding for a monopole antenna are shown in the equations below.

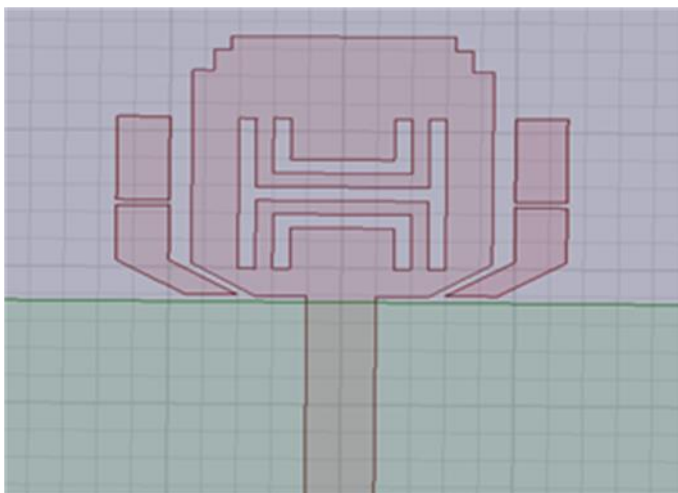


Fig.1 single iteration

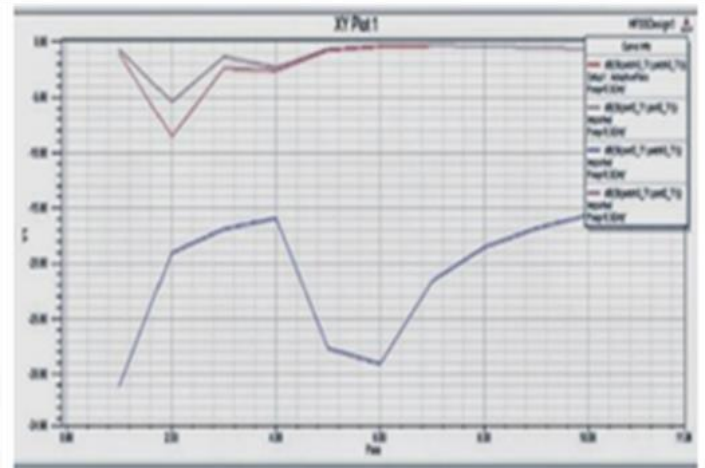


Fig. 2 S11 characteristics of UWB antenna

The CPW's dielectric constant can be computed by equation below:

$$e_{ref} = \frac{e_{rr}+1}{2} \left( \tanh \left[ 0.775 l_n \left( \frac{h}{G} \right) + 1.75 \right] + \frac{Kg}{h} \times [0.004 - 0.7k + 0.01(1 - 0.1e_r)(0.25 + k)] \right) \quad (1)$$

Where,

$$k = \frac{w}{h} + 2G \quad (2)$$

w= breadth of the centre conductor,

h = Layer thickness,

G = Above the conductor and the earth, there is a gap.

The ratio between the first-order elliptic integral to its complement can be calculated using the following formula:

$$Z_{0CPW} = \frac{20\pi}{\frac{\sqrt{e_{ref}K'(k)}}{K(k)}} \quad (3)$$

Where,

$$\frac{K'(k)}{K(k)} = \left[ \frac{\pi}{l_n} \left( 2 \left( \frac{1+\sqrt{k}}{1-\sqrt{k}} \right) \right) \right] \quad (4)$$

$$\frac{K'(k)}{K(k)} = \left[ \frac{\pi}{l_n} \left( 2 \left( \frac{1+\sqrt{k}}{1-\sqrt{k}} \right) \right) \right] \text{ If } 0.707 < k < 1$$

From eqn 4,  $e_{ref} = 2.809$ ,  $Z_{0CPW} = 48\Omega$  are theoretical values for the design parameters including  $r = 4.4$ ,  $h = 1.6\text{mm}$ ,  $w = 2\text{mm}$  and  $G = 0.3\text{mm}$ . It has been done with ultra-wideband, which has a frequency range of 2.4 to 18.6 GHz and 15.6 GHz as a bandwidth. The patch has rectangular radiating elements and an H-slot combined with dual U-slots to successfully implement the dual-band notched characteristics. Using the following equations in 5, it is possible to establish the maximum dimension of the stubs that are H- and U-shaped and positioned in the notches frequency in the central band.

$$L_s = \frac{\lambda_g}{4} \quad (5)$$

$$\lambda_g = \frac{\lambda_0}{\text{Sqrt}\epsilon_r} \quad (6)$$

Where,  $\lambda_g$  represents the wavelength direction  $\lambda_0 = c_0 / \epsilon_r$ ,  $\epsilon_r$  represents the dielectric constant, and  $c_0$  represents the velocity light

Figure 1 depicts a mathematical viewpoint of monopole radio wire having hole sleeves, Figure 2 depicts the S11 characteristics of a UWB radio wire, and Figure 3 depicts the plan of a monopole accepting wires including H-formed stubs. The prototype of receiving wires was created using 37 x 40 x 1.6 MM3 measured FR-4 substrate. With scores at 8.3 GHz (military and radar), and 3.6 GHz (WiMAX) the suggested monopole receiving wire achieved an extensive transmission capability over 16 GHz from 2.1 GHz to 18.2 GHz. In this way, the intentional and replicated outcomes should be the same.

### 3.1 THE MIMO ANTEENA DESIGN

The parallel receiving wire MIMO with two component in Fig. 3 has a 2 mm gap between its M1 component and M2 component ranges. The antenna may be created using a substrate FR-4 with dimensions of 37 x 82 x 1.6mm<sup>3</sup>. Figure 4 shows the S-boundary characteristics of the 2-component

parallel MIMO receiving wire. Because the components of the radio wire are similar to one another, the port-1 s-boundaries, which are S11 and S12, are currently dissected and identified. Dissipating boundary qualities, as seen in port 1, operate between 3.3 to 17.6GHz with an indent around 8.3GHz. The boundary S12 will provide coupling between two components. This coupling should be around - 20 dB, and at repetition 7.6 GHz, it achieves a very dangerous level of detachment. The mathematical viewpoint on MIMO receives wire having two components is shown in Figure 3. The positions of both of the M1 and M2 components are 180° apart but in the opposite direction.

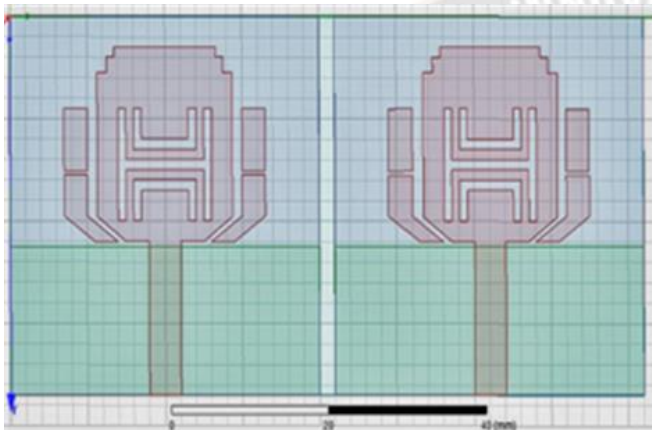


Fig. 3 Collinear MIMO Antenna with two elements

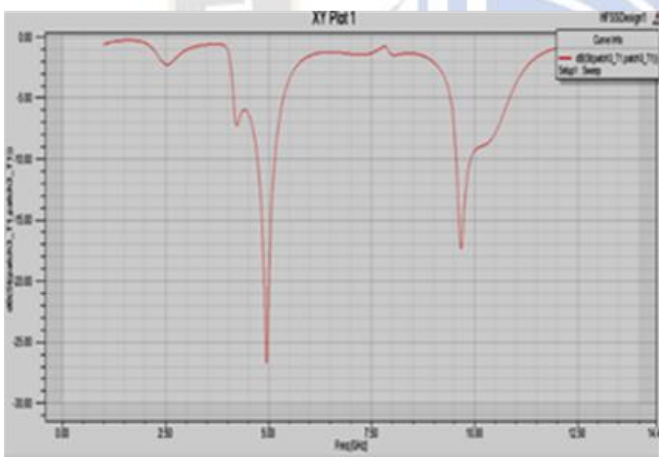


Fig. 4 S-parameter of a Collinear MIMO Antenna with two elements

This kind of receiving wire is moreover on a FR-4 substrate with the sizes 37801.6 mm<sup>3</sup>, and the characteristics of its dispersing boundary are shown in Figure 3. The radio wire's recurrence range spans 2.1 - 18.2 GHz, with scores at 3.6 - 8.3 GHz. Separation between the M1 and M2 elements is greater than 20dB.

The divergence between M1 and M2 elements will progressively reduce when M1 and M2 elements are symmetric to one another, as seen in Fig. 4. Additionally, this radio wire was produced on a FR-4 substrate with dimensions

of 40 80 1.6 MM<sup>3</sup>, and Figure 4 shows its s-boundary characteristics for Port 1. This radio cable operates between 2.1GHz to 16.5GHz and has a frequency range of 3.8GHz to 8.4GHz. It doesn't have a precise -30 dB common coupling. Finally, disengagement is increased by arranging components at an angle of 90 degrees to one another. Figure 5(a) proposes and introduces four element symmetrical MIMO receiving wires. Additionally, this radio cable may be used to improve data transmission for excellent segregation. This MIMO model uses a split ground plane model to reduce coupling between exhibit components. An instance of MIMO radio wire in this model lacks a ground reference, which obstructs the receiving wire. Additionally, the advancement of conduct between two different devices can reduce the radio wire's stability. By using a split ground plane with four components connected by 0.2 mm wide connection lines, this can be avoided.

It is produced on a FR-4 substrate with dimensions of 80 x 80 x 1.6 mm<sup>3</sup> with 4.4 as dielectric constant. The construction of a radio wire is portrayed in figure 5(c), with the recreated and predicted dissipating boundaries S11–S14 are illustrated in figure 5(d). Additionally, this four-component MIMO receive wire contains indents at 3.6 - 8.3GHz and a broad array of impedance transmission speed (S11 – 10 dB) of 17.9GHz between 2.1-20GHz. The divide between (M1, M3) must be more severe as compared to the disengagement among (M1, M2) elements and (M1, M4) elements. The proposed radio wire's typical isolation is greater than -26dB across the whole working reach. In every situation, the characteristics of estimated and replicated boundaries should be the same. Additionally, topology of MIMO radio wire with four elements we suggested is typically applied for UWB uses. Utilizing metamaterial, the suggested antenna is changed for addressing the issue of isolation.

According to antenna survey materials, there are two types of metamaterials: antennas based on MTM or motivated by MTM. The metamaterial's qualities are not present in nature. They contain either negative permeability, or permeability, or both. DNG (Double Negative), MNG (-negative), or ENG (Epsilon Negative) or are used. The foundation is made of MTM-based antennas. The sole MTM unit cell, including the CSRR and SRR (Complementary Split Rings Resonator and Split Ring Resonator). A metamaterial is created. Single-Negative Magnetic is effectively used to reduce electromagnetic coupling between the widely spread prominent monopole antenna parts. SRR, CSRR, and CLL (Capacitive-Loaded-Loops) are typical MTM important structures for the isolation upgrade. The electromagnetic waves from the nearby antenna may become obstructed in a Split Ring Resonator.

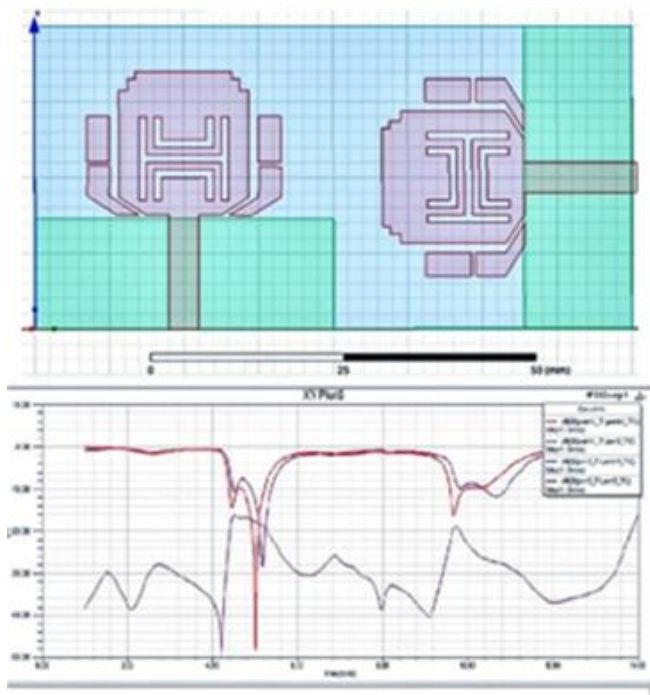


Fig. 5 2 piece orthogonal MIMO antennas placed side by side with S parameters

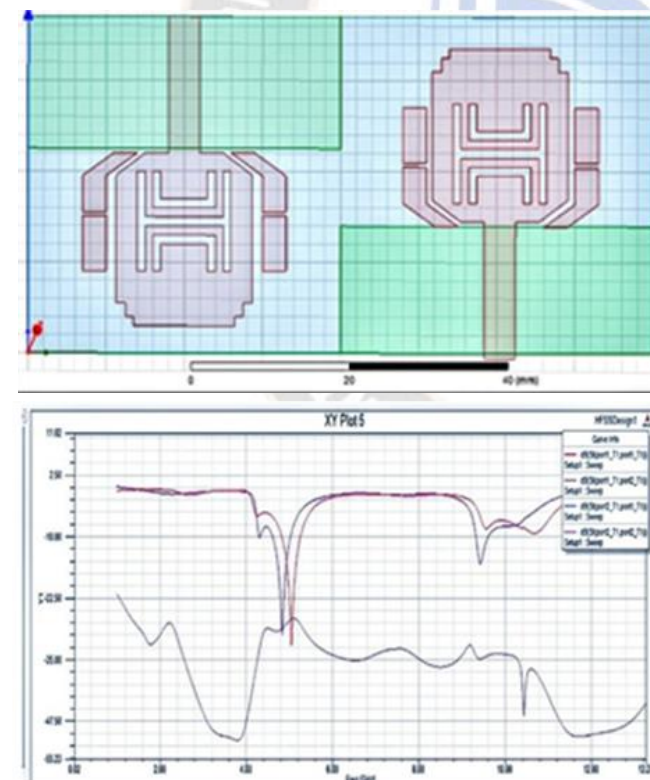


Fig. 6 2 piece orthogonal MIMO antenna S parameters

Below tabulated values show how the proposed antenna is best.

The symmetrical 4-element MIMO antenna used in the suggested concept has ECC values around 0.019. If the altered value of ECC is below or identical to 0.03, the model is

popular one. While the antenna generates an ECC number around 0.05, it is not the suggested antenna. The degree of isolation is also impacted when the ECC level is decreased. Because we wanted to offer an ECC value lower than 0.03, we chose this shape over the f shape. The value of ECC of our suggested antenna is nearly 0.019. The symmetrical 4-element MIMO antenna used in the suggested concept has ECC values around 0.019. While the antenna generates an ECC number around 0.05, it is not the suggested antenna. The degree of isolation is also impacted when the ECC level is decreased. Because we wanted to offer an ECC value lower than 0.03, we chose this shape over the f shape.

PARAMETERS	H	F
SIZE	80*80*16m m3	30*26*106 mm
IMEPEDANCE BANDWIDTH	S11<-10DB(2.4GHZ-18GHZ)	S11<-10DB(3.2GHZ-3.8GHZ) AND S12<-20DB(5.7GHZ-6.8GHZ)
ECC	<0.19	<0.03
DIRECTIVITY GAIN	~10	9.8
PEAK GAIN	5.9	5.08
RADIATION EFFICIENCY	82%	80%
MUTUAL COUPLING	<-20DB	<-20DB
ISOLATION	SPLIT RING RESONATOR	ELEPTICAL SLOT AND RECTANGULAR PARASATIC STRIPS CONTRIBUTE TO HIGH ISOLATION
FEEDING	CWP	CWP
SUBSTRATE	FR-4	FR-4

#### IV. MIMO PERFORMANCE PARAMETERS

##### 4.1 DISTRIBUTION OF SURFACE CURRENT:

The four-element antenna's distributions of surface current are taken into account at notch frequencies 3.6 and 8.3 GHz and within the operation range of 5.8 and 10 GHz.

##### 4.2 RADIATION PATTERNS:

Figures 8 and 9 show two-dimensional radiation designs for two-component MIMO radio wires at 10 and 5.8 GHz in a variety of planes, including xy, yz, and zx planes. Where the XY plane, or receiving wire plane, is where the two-component MIMO receiving wires operates. Lastly, co-polarization succeeds at the Gain-phi value while co-polarization succeeds at the Gain-theta value.

The end-fire bearing has two basic bars, with the largest ones transmitting at 45 or 135 degree. The boldness of experimental and replicated results validates the design's correctness. The

majority of radiation designs are high frequency in nature, and the ability to distinguish between co-polarization and cross-polarization is the weakest.

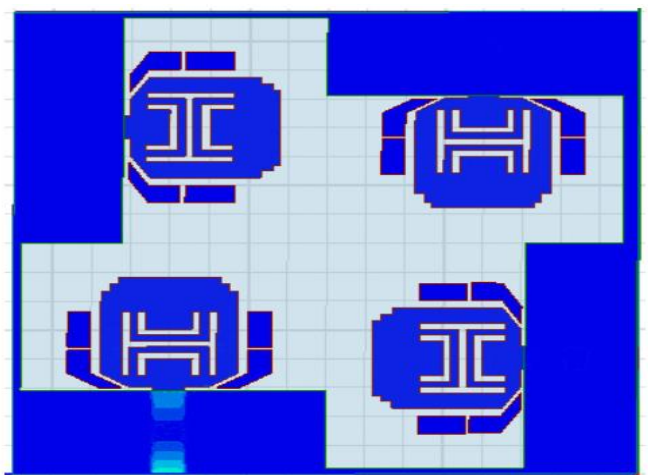
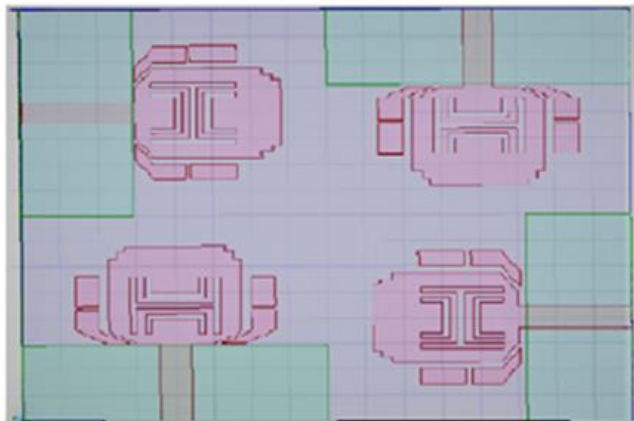


Fig: 8 MIMO Antenna - Distribution of surface current at 3.7 GHz

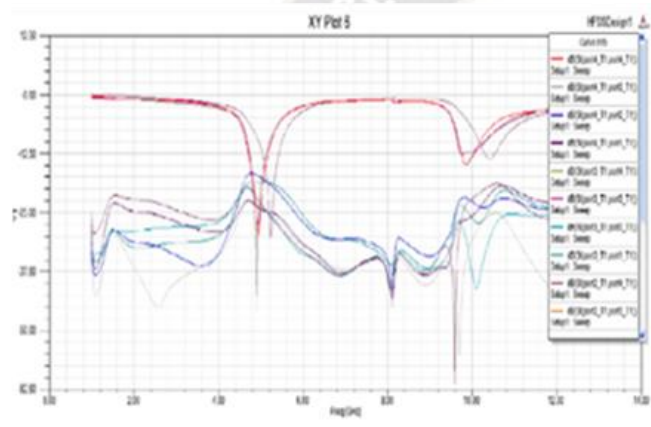


Fig. 7 MIMO Antenna with Four elements and split ground

### 4.3 ENVELOP CORRELATION COEFFICIENT (ECC):

As far as the connection in figure 12 is concerned, diversity among the suggested MIMO radio wire with 2 element is considered. For every MIMO radio wire, the ECC should be less than 0.5 to demonstrate reasonable variation. Co-relation of MIMO wire with port 1 and 2 can achieve irradiation designs are matched in circumstance (7). As demonstrated in the lower portion of Fig. 12, both imitated and tested ECC esteems tend to be extremely close to 0.02 throughout the entire 5G range while differing at indents.

### DG (Diversity Gain):

The DG, which is characterised as

$$D_G = 10\sqrt{1 - ECC^2}$$

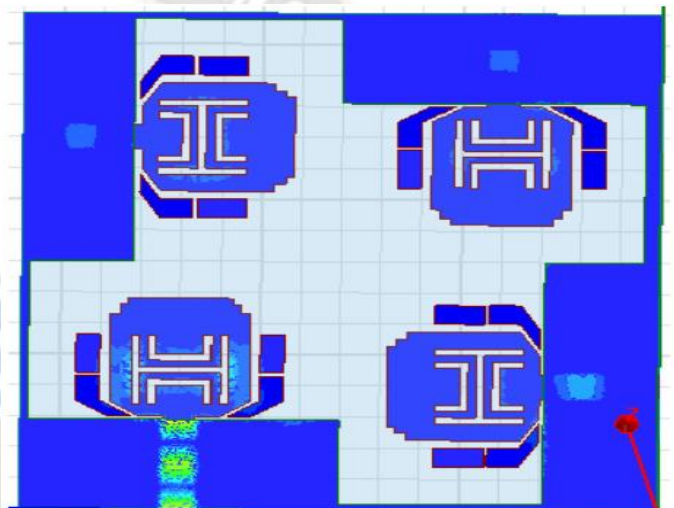


Fig: 9 MIMO antenna surface current at 5.9 GHz

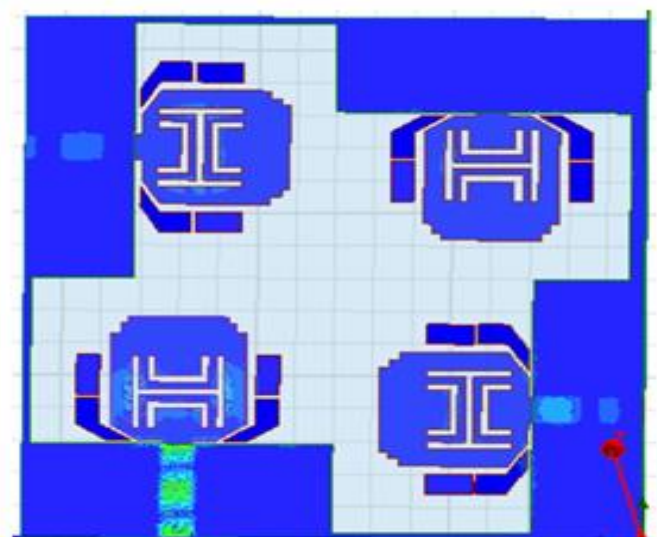


Fig:10 At 10GHz, MIMO antennas surface current distribution



The antenna directivity is depicted in figure 13. In terms of directivity, the suggested design outperforms existing designs such as CPW, CST, and ESG by 3.45%, 5.95%, and 7.48%, respectively.

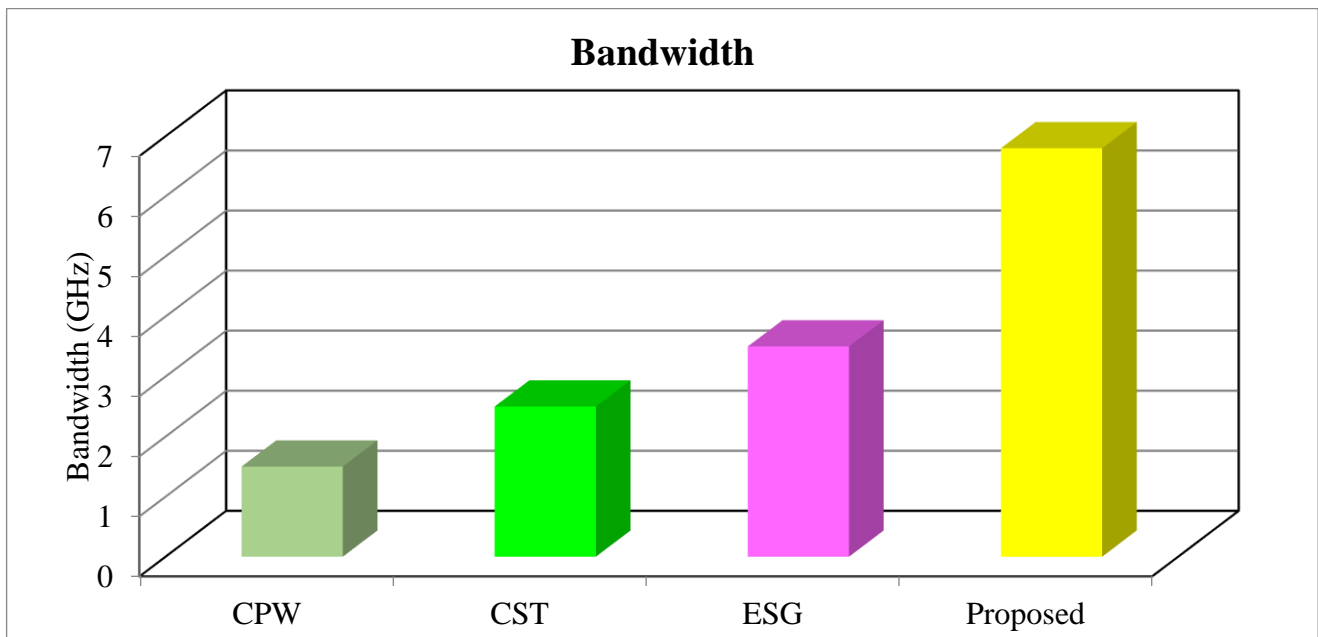


Figure 14: Antenna Bandwidth

The antenna bandwidth (GHz) is depicted in figure14. The proposed design outperforms the existing designs, such as CPW, CST, and ESG, in terms of bandwidth by 6.75, 5.77, and 8.94%, respectively.

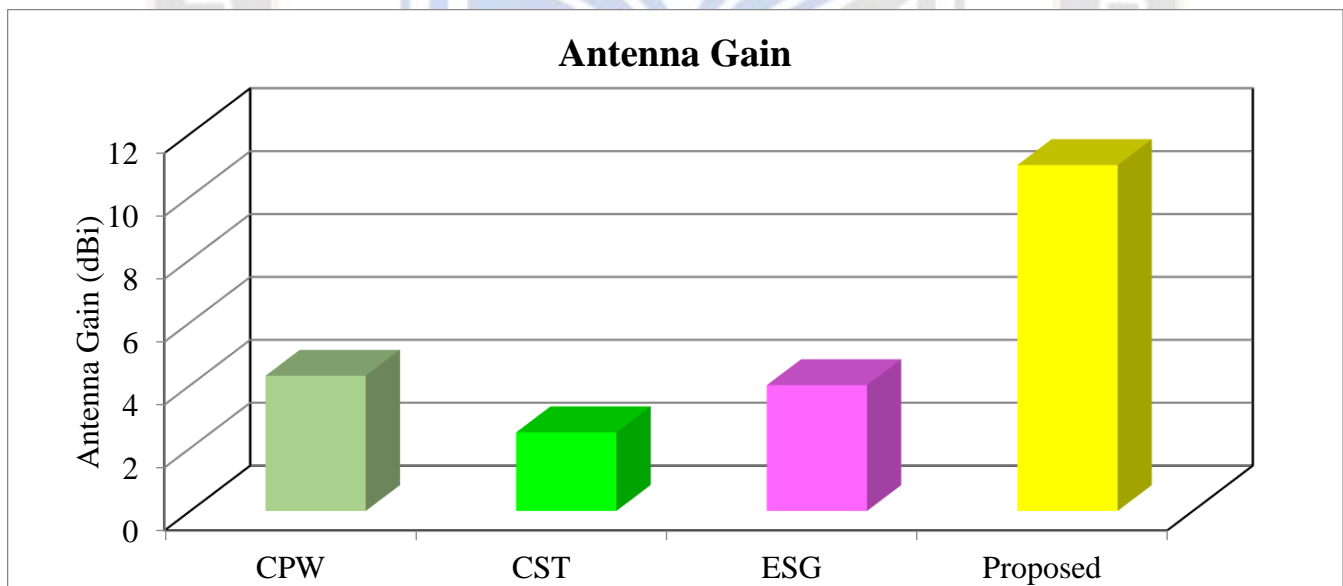


Figure 15: Antenna gain (dBi)

The antenna gain (dBi) is depicted in figure 15. The proposed design outperforms the existing designs, including CPW, CST, and ESG, in terms of antenna gain, by 4.72, 8.0, and 7.5 percent, respectively.

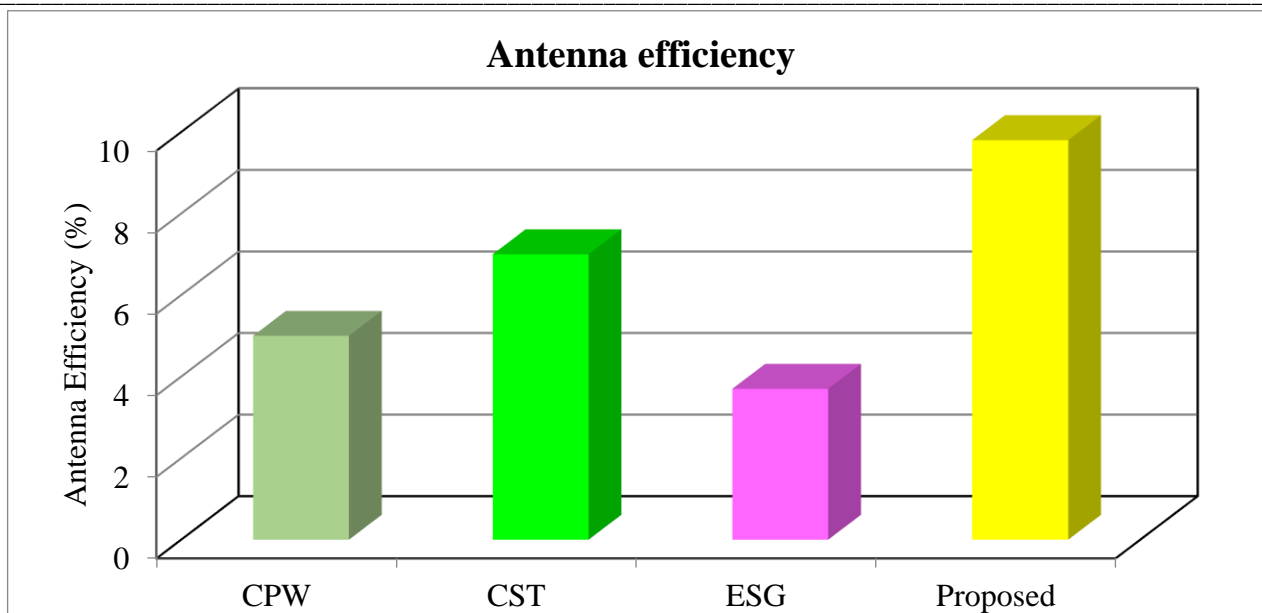


Figure 16: Antenna efficiency (%)

The antenna efficiency is depicted in figure 16. The proposed design outperforms the existing designs, such as CPW, CST, and ESG, in terms of antenna efficiency by 7.95%, 5.87%, and 4.09%, respectively.

## V. CONCLUSION

For UWB applications, orthogonal MIMO antennas with four elements are recommended. By installing H & U slots containing gaps sleeves on the monopole antenna, a band with a pair of notches was utilised in this hypothetical case. I discovered antenna specifications here. It is possible to design it using the FR4 substrate's dimensions. Following the simulation, I attained various frequencies. A few antenna parameters, including the DG, ECC, power distribution, S11 features, far-field radiation features, plus a few other radiation patterns, were designed by me. With notch from 3.3 - 4.3GHz, from 8.2 - 8.7GHz, the suggested MIMO antenna's bandwidth of impedance (S11-10dB) spans the frequency arrays of 2.4 to 20GHz. The acquired notches may be appropriate for WiMAX and radar/ military applications. Additionally, the Mutual coupling is below -19 dB when surrounded by the environment. The suggested antenna's maximum gain, which appears in the desired working band and that adeptly greater electromagnetic radiation of the antennas is in excess of 82% at the number of notches, is here another criterion that satisfies the needed measurement. This antenna is highly diverse, has a low ECC of 0.019, and is well-isolated. The proposed antenna achieves steady gain, directed patterns of radiation, that bandwidth of impedance using twofold notches, and this is supported by research on the performance of the MIMO antenna. This suggested antenna made use of four identical, symmetrical MIMO elements. It is

therefore possible to infer, after taking into account all the aforementioned factors, that the suggested MIMO antenna, which consists of four elements, is appealing and appropriate and 5G applications including notches at WIFI and WiMAX for military/radar applications as well as bio-medical applications.

### Compliance with Ethical Standards

#### Conflict of interest

The authors declare that they have no conflict of interest.

#### Human and Animal Rights

This article does not contain any studies with human or animal subjects performed by any of the authors.

#### Informed Consent

Informed consent does not apply as this was a retrospective review with no identifying patient information.

**Funding:** Not applicable

**Conflicts of interest Statement:** Not applicable

**Consent to participate:** Not applicable

**Consent for publication:** Not applicable

#### Availability of data and material:

Data sharing is not applicable to this article as no new data were created or analyzed in this study.

**Code availability:** Not applicable

## REFERENCES

- [1] L.Liu,S.W.Cheung, and T.I.Yuk,“Compact MIMO antenna for portable devices in UWB applications,”*IEEETrans.Antennas Propag.*, vol.61,no.8, pp.4257–4264, Aug.2013.
- [2] J.-Y.Deng,L.-X.uo and X.-L.Liu,“An ultra-wide band MIMO antenna with a high isolation,”*IEEE Antennas Wireless Propag.Let.vol.15*,pp. 182–185,2016.
- [3] W.A.E.Aliand A.A.Ibrahim,“A compact double-sidedMIMO antenna with an improve disolation for UWB applications,”*AEU-Int.J. Electron Common.vol.82*,pp. 7–13,Dec.2017.
- [4] T.-C. Tang and K.-H.Lin, “An ultra-wideband MIMO antenna with dual band-notched function,” *IEEE Antennas Wireless Propag.Lett.*,vol. 13,pp.1076–1079,2014.
- [5] H. Huang, Y. Liu, and S. Gong, “Uniplanar differentially driven UWB polarization diversity antenna withband-notched characteristics,”*Electron. Let.vol. 51*,no. 3,pp. 206–207,Feb.2015.
- [6] Gore, S. ., Dutt, I. ., Dahake, R. P. ., Khodke, H. E. ., Kurkute, S. L. ., Dange, B. J. . and Gore, S. . (2023) “Innovations in Smart City Water Supply Systems ”, *International Journal of Intelligent Systems and Applications in Engineering*, 11(9s), pp. 277–281. Available at: <https://ijisae.org/index.php/IJISAE/article/view/3118>.
- [7] L. Liu, S. W. Cheung, and T. I. Yuk, “Compact MIMO antenna for portable UWB applications with band-notched characteristic,”*IEEE Trans. Antenna naps Propag.*, vol. 63, no.5, pp.1917–1924, May2015.
- [8] S. Rajkumar, A. Anto Amala, and K.T. Selvan, "Isolation enhancement of UWB MIMO antenna using molecular fractal structure," *ELECTRONICS LETTERS*, Vol. 55, No. 10, May 2019, pp. 576–579.
- [9] Ahmed S. Eltrass and Nahla A. Elborae, "New Design of UWB-MIMO Antenna with Improved Isolation and Dual-Band Rejection for WiMAX and WLAN Systems," *IET Microwaves, Antennas & Propagation*, Vol. 13 Iss. 5, pp. 683-691.
- [10] Li Ying Nie, Xian Qi Lin, Zi Qiang Yang, Jin Zhang, and Bao Wang, "Structure-Shared Planar UWB MIMO Antenna with High Isolation for Mobile Platform," *IEEE TRANSACTIONS ON ANTENNAS AND PROPAGATION*, VOL. 67, NO. 4, APRIL 2019.
- [11] Tholkapiyan, M. ., Ramadass, S. ., Seetha, J. ., Ravuri, A. ., Vidyullatha, P. ., Shankar S., . S. . and Gore, S. . (2023) “Examining the Impacts of Climate Variability on Agricultural Phenology: A Comprehensive Approach Integrating Geoinformatics, Satellite Agrometeorology, and Artificial Intelligence”, *International Journal of Intelligent Systems and Applications in Engineering*, 11(6s), pp. 592–598. Available at: <https://ijisae.org/index.php/IJISAE/article/view/289>.
- [12] Zhenya Li, Chengyu Yin, and Xiaosong Zhu "Compact UWB MIMO Vivaldi Antenna with Dual Band-Notched Characteristics" *IEEE Access*, VOLUME 7, 2019.
- [13] Zhijun Tang et. al. "Compact UWB-MIMO Antenna with High Isolation and Triple Band-Notched Characteristics" *IEEE Access*, VOLUME 7, 2019.
- [14] Syed S. Jehangir and Mohammad S. Sharawi “A Wideband Sectoral Quasi-Yagi MIMO Antenna System with Multibeam Elements” *IEEE Transactions on Antennas and Propagation*, VOL. 67, NO. 3, March 2019.
- [15] Dange, B. J. ., Mishra, P. K. ., Metre, K. V. ., Gore, S. ., Kurkute, S. L. ., Khodke, H. E. . and Gore, S. . (2023) “Grape Vision: A CNN-Based System for Yield Component Analysis of Grape Clusters ”, *International Journal of Intelligent Systems and Applications in Engineering*, 11(9s), pp. 239–244. Available at: <https://ijisae.org/index.php/IJISAE/article/view/3113>.
- [16] Libin Sun set. al. "A Compact Planar Omni directional MIMO Array Antenna With Pattern Phase Diversity Using Folded Dipole Element" *IEEE Transactions on Antennas and Propagation*, VOL. 67, NO. 3, March 2019.
- [17] Anping Zhao and Zhouyou Ren “Size Reduction of Self-Isolated MIMO Antenna System for 5G Mobile Phone Applications” *IEEE Antennas and Wireless Propagation Letters*, VOL. 18, NO. 1, January 2019.
- [18] Bing-Jian Niu and Jie-Hong Tan "Compact SIW cavity MIMO antenna with enhanced bandwidth and high isolation" *ELECTRONICS LETTERS* 30th May 2019 Vol. 55 No. 11 pp. 631–632.
- [19] Sreenath Reddy Thummalur, Rajkishor Kumar, Raghvendra Kumar Chaudhary “Isolation and frequency reconfigurable compact MIMO antenna for wireless local area network applications” *IET Microwaves, Antennas & Propagation*, 2019, Vol. 13 Iss. 4, pp. 519-525T
- [20] Tiwari, R.N., Singh, P., Kanaujia, B.K. and Srivastava, K., 2019. Neutralization technique based two and four port high isolation MIMO antennas for UWB communication. *AEU-International Journal of Electronics and Communications*, 110, p.152828.
- [21] Dkiouak, A., Zakriti, A., Elftouh, H. and Mchbal, A., 2020. Design of CPW-fed MIMO antenna for ultra-wideband communications. *Procedia Manufacturing*, 46, pp.782-787.
- [22] Naktong, W. and Ruengwaree, A., 2020. Four-port rectangular monopole antenna for UWB-MIMO applications. *Progress In Electromagnetics Research B*, 87, pp.19-38.
- [23] Sediq, H.T., Nourinia, J., Ghobadi, C. and Mohammadi, B., 2022. An epsilon-shaped fractal antenna for UWB MIMO applications. *Applied Physics A*, 128(9), pp.1-15.
- [24] Sathiyapriya, T., Gurunathan, V., Dhanasekar, J. and Teresa, V.V., 2022. Design of High Isolation MIMO Antennas for Ultra-Wide Band Communication. In *Evolution in Signal Processing and Telecommunication Networks* (pp. 161-170). Springer, Singapore.
- [25] V. S. Bhaskar and E. L. Tan, "Design of dual-band omni directional planar microstrip antenna using Giel is curves, "in *Proc. IEEE Int. Symp. Antennas Propag. North Amer. Radio Sci.Meeting*, Montreal, QC, Canada, Jul.2020, pp.309-310.